Sādhanā Vol. 33, Part 3, June 2008, pp. 329–338. © Printed in India

Micro and macro contact mechanics for interacting asperities

M RAMESH*, SATISH V KAILAS and K R Y SIMHA

Department of Mechanical Engineering, Indian Institute of Science, Bangalore 560 012
e-mail: mramesh@mecheng.iisc.ernet.in

Abstract. Contact of rough surfaces at micro and macro scales is studied in this paper. The asperities at micro scale are characterised by small radius of curvature whereas the waviness is characterised by large radius of curvature. When two rough surfaces come in contact, on the micro scale, of asperities contacts in a very small area leave large gaps between the surfaces; whereas on the macro scale the surfaces conform to each other under the application of load without gaps. Contact at micro scale is modelled by superposition of Hertzian stress fields of individual asperity contacts and the waviness at macro scale is modelled as a mixed boundary problem of rough punch indentation where displacements of uneven profile are prescribed along the region of contact. In both the cases for simplification the roughness is assigned to one surface making the other surface perfectly flat an assumption often made in contact mechanics of rough bodies.

The motivation for modelling the asperities at micro scales comes from the preliminary results obtained from photoelastic experiments. Numerical results are presented based on the analytical results available for Hertzian contacts. The motivation for modelling the asperities at macro scales comes from the results available in literature for flat contacts from solving mixed boundary elasticity problems. A condition of full stick is assumed along the contact which is a common assumption made for rough contacts. The numerical results are presented for both the cases of rough contact at micro and macro scales.

Keywords. Hertzian contact; interaction stress field; photoelasticity; shrink-fit; rough hub.

1. Introduction

Design of contact between engineering components is challenging and important, since unexpected failures well below expected life of the components are often observed, for example, due to fretting fatigue. Besides the geometry of the contacting bodies, the roughness of the surfaces under contact plays a major role in deciding the severity of contact stresses. The surface roughness leads to interlocking of asperities at micro scale resulting in friction between

*For correspondence

the contacting surfaces. Friction in general is expected to increase with the surface roughness and can be reduced appreciably by the use of lubricants and soft coatings.

The asperities at micro scale are characterised by small radius of curvature and when two rough surfaces come into contact (figure 1a), the contact at micro scale is characterised by a large number of asperities making contacts in a very small area leaving large gaps between the surfaces. At macro scale there is a possibility of uneveness in the surface formed during manufacturing process. This waviness in surfaces is in general characterised by large radius of curvature and when two such surfaces come into contact (figure 1c) they conform to each other under the application of load without leaving any appreciable gap between the surfaces.

While asperity contacts at micro scale are often detrimental the waviness at macro scale could be advantageous at some instances as it accomodates the local strains which otherwise would create large contact stresses especially in cylindrical contacts. In order to take advantage of these features, it is necessary to design such waviness based on rigorous contact stress analyses and which remains widely unexplored.

Contact at micro scale is modelled by superposition of Hertzian stress fields of individual asperity contacts and the waviness at macro scale is modelled as a mixed boundary problem of rough punch indentation where displacements of uneven profile are prescribed along the region of contact. In both the cases for simplification the roughness in both surfaces is accumulated in to one surface making the other surface perfectly flat an assumption often made in contact mechanics of rough bodies (figures 1b and d).

Since contact of rough surfaces at microscale is characterised by large number of very small contacts at asperities separated from each other leaving large gaps between the surfaces, it is possible to superpose the stresses due to the contact of each asperity to obtain the state of stress developed due to the contact. Hence assuming the other surface to be made of large number of individual indenters simultaneously indenting a surface (assumed to be half-plane) at multiple regions, the state of stress developed can be determined if the load acting on each of the assumed individual indenters and the contact areas under each indenter is known. The friction in general caused by the interlocking of irregularities of the surface at the micro scale. Hence at micro scale the concept of friction fails and therefore for analysis the surfaces is considered to be frictionless, inspite of the fact that there could be a possible adhesive forces at atomic levels providing shear tractions.

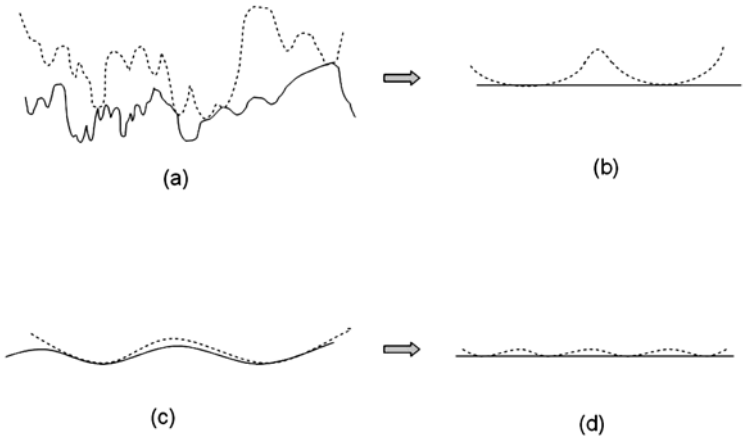

Figure 1. Micro and macro level contacts.

At macro scale the contact of uneven surfaces which will conform to each other under load can be modelled as punch of uneven profile indenting a surface. The surface away from the punch is considered to be traction free. This problem of elasticity can be modelled in terms of mixed boundary problem prescribing the uneven surface profile under the punch and prescribing traction free condition in the remaining surface. The evolution of friction due to locking of asperities at microscale is often modelled at a macro scale assuming a coefficient of friction. However, a condition of full stick is assumed at the contact interface.

In this paper, the analysis of contact of rough surface at both the scales are attempted in different contexts. The rough contact at micro scale is considered in terms of interaction of Hertzian contact stress fields without the presence of any shear tractions. On the other hand, the problem of contact of uneven surfaces is analysed by formulating a mixed boundary elasticity problem prescribing the displacements of uneven profiles within the assumed region of contacts.

2. Interacting Hertzian micro contact stress fields

Based on the above discussions, it is possible to model the problem of asperity contacts of rough surfaces in terms of individual indenters each representing an asperity, indenting an half-plane. Because of the relative heights between the individual profiles the number of asperities making contact in general increases with load. Further, the important issue of the analysis is that the interaction of contact stress fields which is focussed in this paper. In this context a problem of asperity contact at micro scale is modelled as two adjacent indenters indenting a half-plane. The load acting on each indenter is assumed to be equal and the interaction of Hertzian contact stress field is analysed.

The predictions from Hertz theory applied to the 2D contact of a disc over half-plane is that the pressure distribution is semi-elliptical $p(x) = p_0\sqrt{1 - \left(\frac{x}{a}\right)^2}$, with p_0 being the peak pressure at the middle of contact and $2a$ being the contact length. p_0 and a are related by $p_0 = \frac{2P}{\pi a}$ where, P is the applied load. The semi-contact length a is related to the radius of the indenter R, the load applied P and the effective modulus of the contacting bodies E as $a = \sqrt{\frac{4PR}{\pi E}}$ (Johnson 1985). The important implication of the Hertz theory is that maximum shear stress reaches its peak directly below the contact at a distance of about $0{\cdot}78a$.

The Hertzian solution can be extended to obtain near contact stress fields of rough contacts, by assuming the asperity to be an indenter and the other body to be a smooth half-plane. This solution is valid only near the contact and it may not be accurate far away from the contact because of actual component geometry. However, since the stress field developed in a region very near to the contact is crucial to operate any mechanism of wear and crack initiation at microscopic level the solution obtained could provide clues to predict these micro mechanisms.

When rough surfaces make contact the indentation will occur at more than one place. Hence it is important to study the interaction between the individual contact stress fields. Rajendrakumar & Biswas (1996) discussed the non-Hertzian contact of rough indenter indenting a smooth half-plane. In such a case the load acting on each contact region will be different. If load acting on each contact is known then the problem of indentation at multiple places can be studied by superposing the stress fields due to individual contact. The interaction problem becomes important when the contact areas lie close to each other. The problem of a half-plane

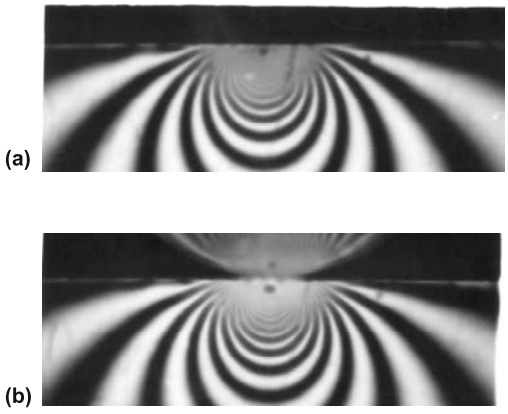

Figure 2. Photoelastic experiment. **(a)** Isochromatics (rigid indenter). **(b)** Isochromatics (elastic indenter).

indented by two indenters with circular profiles very close to each other is considered in this paper. Assuming the load to be same on both the indenters, the interacting contact stress field is obtained by superposing the individual contact stress field.

Preliminary photoelastic experiments were conducted to simulate the Hertzian contact stress fields with a disc indenting a plate whose dimensions are sufficiently larger than the contact area so that the half-plane assumptions are valid. The plate was made of Araldite which is a common photoelastic material. Two experiments were conducted, one with steel disc and other with araldite disc for indenting the plate. Figure 2 shows the fringe patterns corresponding to steel and araldite discs. The small dark spot near the surface is called as the eye in the sequel. This eye gives the location of the maximum shear stress mentioned earlier.

Figure 3a shows the schematic of loading arrangement along with the specimen and indenter for double indentation configuration. The indenters shown in figure are machined from a circular disc so that the contact profiles are circular. The indenters are clamped in a metal plate so that the load applied to the metal plate is distributed equally to the two contact regions. They were cut in a manner to achieve different spacings between the contact, by aligning the opposite sides of the cut-outs. While applying the load care was taken to minimize the out-of-plane bending of the plate.

The photoelastic fringes obtained for two different cut-out spacing with dark field is shown in figures 3b and 3c. The fringes show the Hertzian fringe pattern along with the eye corresponding to each contact. Further, the interaction between the stress fields is clearly demonstrated. Also forms a third eye along the mid-plane between the two contacts. This shows the presence of a peak or valley in the distribution of maximum shear stress. The magnitude of the maximum shear stress level is important if it is comparable to that of the Hertzian eye. However, the fringe order shows that magnitude of stress level is lower than that of Hertzian eye. The slight tilting of the fringes with respect to the horizontal is due to the interaction of the contact stresses.

2.1 *Theoretical analysis*

Motivated by the results of the experiment, the problem of double indentation is analysed by superposing the stress fields due to individual Hertzian contacts. Closed form solutions for the stresses are given in Johnson (1985); Hills *et al* (1993) for a single Hertzian contact. These results are utilised for superposition to achieve the interaction stress field. Figure 4 shows

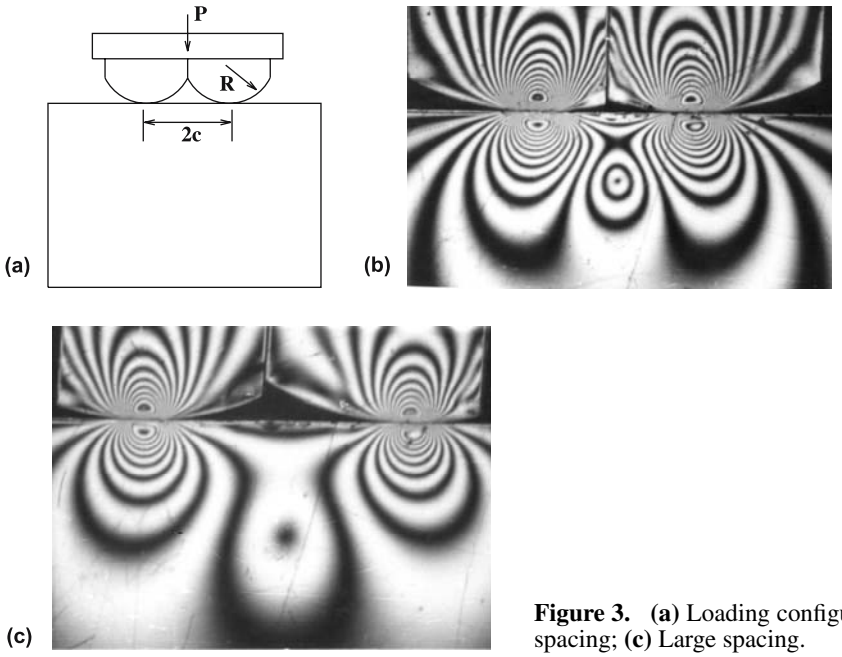

Figure 3. **(a)** Loading configuration; **(b)** Small spacing; **(c)** Large spacing.

that, the obtained fringe patterns correspond with the experimental results. The formation of third eye is predicted. Since this third eye is found to be an isotropic point under hydrostatic compression. Thus the results demonstrate that the superposition of the individual stress fields to obtain the interaction stress field is valid.

It can be stated from the results that as the distance between the contacts decreases the fringes of higher order start interacting.

3. Contact of surfaces with uneven profiles at macro scale

The contact of surfaces with uneven profiles at a macro scale is considered in this section. Since this analysis is for macro scale, the assumption of half-plane is no longer valid. Hence the actual geometry of the component becomes important. For analysis a hub shrink-fitted onto a cylindrical shaft is considered.

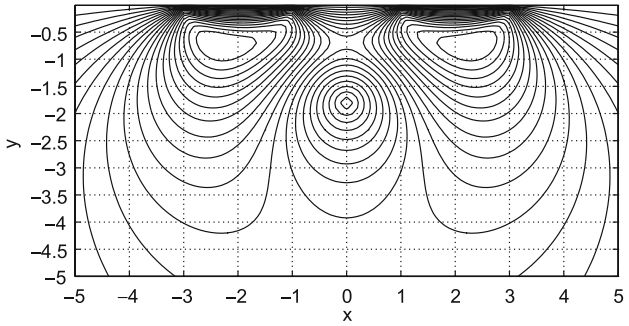

Figure 4. Contours of maximum shear stress for a half-plane indented by two spherical indenters.

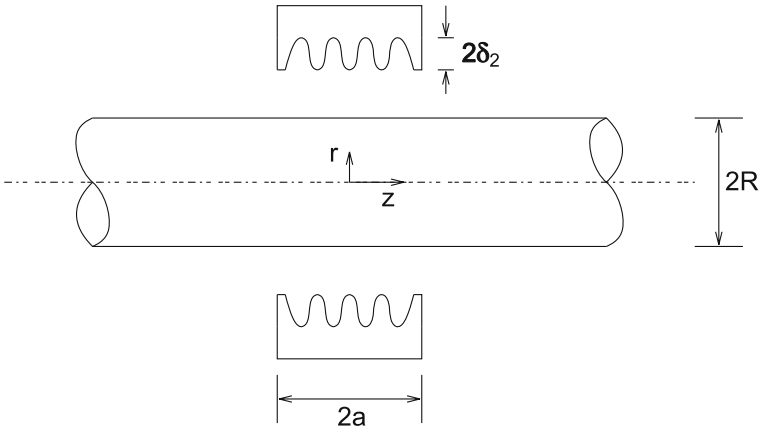

Figure 5. Cylinder with an axisymmetric hub having sinusoidal profile.

Shrink-fitted components often fail by fatigue due to growth and propagation of cracks initiated at the contact interface by fretting. The stress analysis of shrink-fits has been discussed in Conway & Farnham (1967); Spillers (1964); Tranter & Craggs (1945). Yau & Cakmak (1966) discussed the indentation of homogenous hollow cylinder with punches of different profiles assuming the contact to be frictionless. The analysis of cylinder shrink-fitted to a flat hub assuming slipless condition is discussed in Yau (1967). The analysis is extended in this paper assuming the surface of hub to be uneven instead of flat. The case of full stick is considered as is the case of any rough contact. Surface roughness of the hub is modelled by assuming sinusoidal variation of the profile.

Consider a solid cylinder of radius R made of linear elastic material shrink-fitted to an axisymmetric rigid hub with sinusoidally varying profile (figure 5). The length of the hub making the contact is taken to be $2a$. The a/R ratio becomes important when the ratio is small. For larger ratio ($a/R \gg 1$) the problem can be simplified to that of Lame problem. Hence a small value of $a/R = 0{\cdot}5$ is chosen for analysis. The ends of the hub are assumed to be sharp leading to singular stresses.

3.1 *Formulation*

The solution for the Love stress function in the fourier space as explained in 'Near surface stress analysis strategies in axisymmetric fretting' (in this issue)

$$\overline{\Phi} = A_1 f_1(\xi r) + A_2 f_2(\xi r). \tag{1}$$

The expressions for $f_i(\xi x_2)$ are

$$f_1(\xi r) = \frac{1}{\xi^2}\frac{I_0(\xi r)}{I_0(\xi R)} \tag{2}$$

$$f_2(\xi r) = \frac{1}{\xi^2}\frac{\xi r I_1(\xi r)}{I_0(\xi R)}, \tag{3}$$

where R is the radius of the cylinder. The stresses and displacements at the surface are

$$\overline{\tau}_{rz} = A_1(\xi)p_1 + A_2(\xi)p_2 \tag{4}$$

$$\overline{\sigma}_r = A_1(\xi)p_3 + A_2(\xi)p_4 \tag{5}$$

$$\overline{u}_r = A_1(\xi)a_{11} + A_2(\xi)a_{12} \tag{6}$$

$$\overline{u}_z = A_1(\xi)a_{21} + A_2(\xi)a_{22}, \tag{7}$$

where the expressions for p_i and a_{ij} are

$$p_1 = \xi \frac{I_1(\xi R)}{I_0(\xi R)} \tag{8}$$

$$p_2 = \xi \left[2(1-\nu)\frac{I_1(\xi R)}{I_0(\xi R)} + \xi R \right] \tag{9}$$

$$p_3 = \frac{1}{R}\frac{I_1(\xi R)}{I_0(\xi R)} - \xi \tag{10}$$

$$p_4 = -\xi \left[\xi R \frac{I_1(\xi R)}{I_0(\xi R)} + 1 - 2\nu \right] \tag{11}$$

$$a_{11} = -\frac{1+\nu}{E}\frac{I_1(\xi R)}{I_0(\xi R)} \tag{12}$$

$$a_{12} = -\frac{1+\nu}{E}\xi R \tag{13}$$

$$a_{21} = \frac{1+\nu}{E} \tag{14}$$

$$a_{22} = \frac{1+\nu}{E}\left[\xi R \frac{I_1(\xi R)}{I_0(\xi R)} + 4(1-\nu) \right]. \tag{15}$$

Rewriting the unknown functions A_1 and A_2 by the unknown stresses at the surface from eqs. 4 and 5 as

$$A_1(\xi) = \frac{1}{\Delta_1}\left[p_4\overline{\tau}_{rz} - p_2\overline{\sigma}_r \right] \tag{16}$$

$$A_2(\xi) = -\frac{1}{\Delta_1}\left[p_3\overline{\tau}_{rz} - p_1\overline{\sigma}_r \right] \tag{17}$$

with

$$\Delta_1 = p_1p_4 - p_2p_3. \tag{18}$$

We obtain the following expressions for the displacements at the surface

$$\overline{u}_r = k_1\overline{\tau}_{rz} + k_2\overline{\sigma}_r \tag{19}$$

$$\overline{u}_z = k_3\overline{\tau}_{rz} + k_4\overline{\sigma}_r, \tag{20}$$

where k_i are listed as

$$k_1 = [-a_{12}p_3 + a_{11}p_4]/\Delta_1 \tag{21}$$

$$k_2 = [a_{12}p_1 - a_{11}p_2]/\Delta_1 \tag{22}$$

$$k_3 = [-a_{22}p_3 + a_{21}p_4]/\Delta_1 \tag{23}$$

$$k_4 = [a_{22}p_1 - a_{21}p_2]/\Delta_1. \tag{24}$$

Expressing the stresses at the surface along the contact interface (at $r = R$, $|z| \leq a$) as

$$\sigma_r(z) = \sum_{m=1}^{\infty} a_m \frac{\cos\left[(2m-2)\cos^{-1}\frac{z}{a}\right]}{\sqrt{a^2 - z^2}} \tag{25}$$

$$\tau_{rz}(z) = \sum_{n=1}^{\infty} b_n \frac{\cos\left[(2n-1)\cos^{-1}\frac{z}{a}\right]}{\sqrt{a^2 - z^2}}, \tag{26}$$

where a_m and b_n are unknown constants which are to be determined from the boundary conditions. The surface is stress-free away from contact i.e. $\sigma_r(z) = \tau_{rz}(z) = 0$ for $|z| > a$. The above expressions in the fourier space become

$$\overline{\sigma}_r = (-1)^{m-1}\frac{a_m}{2}J_{2m-2}(\xi a) \tag{27}$$

$$\overline{\tau}_{rz} = (-1)^n \frac{b_n}{2}J_{2n-1}(\xi a). \tag{28}$$

Substituting above equations in to equations 19 and 20

$$u_r(z) = \frac{1}{\pi}\sum_{n=1}^{n=\infty} b_n(-1)^n R_{1n}(z) + \frac{1}{\pi}\sum_{m=1}^{m=\infty} a_m(-1)^{m-1}R_{2m}(z)$$

$$u_z(z) = \frac{1}{\pi}\sum_{n=1}^{n=\infty} b_n(-1)^n R_{3n}(z) + \frac{1}{\pi}\sum_{m=1}^{m=\infty} a_m(-1)^{m-1}R_{4m}(z), \tag{29}$$

where

$$R_{1(3)n}(z) = \int_0^{\infty} k_{1(3)}J_{2n-1}(\xi a)\cos(\sin)(\xi z)d\xi \tag{30}$$

$$R_{2(4)m}(z) = \int_0^{\infty} k_{2(4)}J_{2m-2}(\xi a)\cos(\sin)(\xi z)d\xi. \tag{31}$$

The boundary conditions are:

- for $|z| \leq a$, $u_r = -\delta_1 - \delta_2\cos(4\pi\frac{z}{a})$ and $u_z = 0$ (full stick)
- for $|z| \geq a$, $\sigma_r = \tau_{rz} = 0$ (traction free).

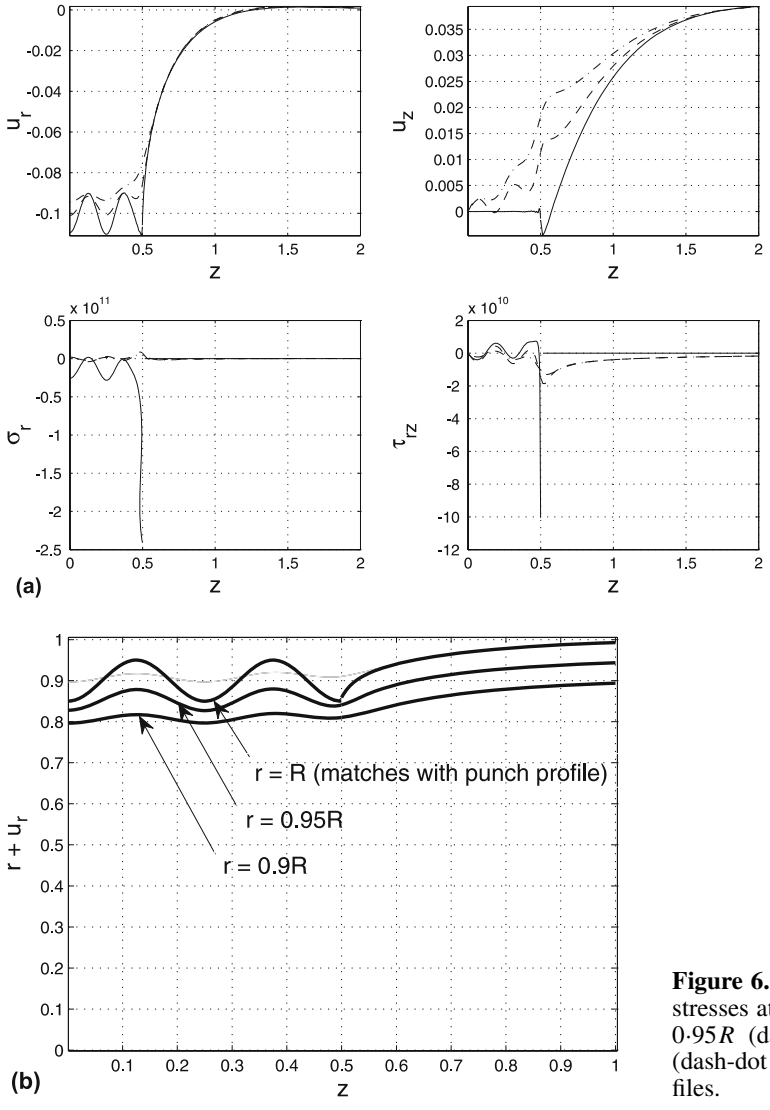

Figure 6. **(a)** Displacements and stresses at $r = R$ (solid line), $r = 0{\cdot}95R$ (dashed line), $r = 0{\cdot}9R$ (dash-dot line). **(b)** Deformed profiles.

The traction free condition away from contact is already ensured. The displacements within the contact is ensured by

$$\frac{1}{\pi}\sum_{n=1}^{n=\infty} b_n(-1)^n R_{1n}(z) + \frac{1}{\pi}\sum_{m=1}^{m=\infty} a_m(-1)^{m-1} R_{2m}(z) = -\delta_1 - \delta_2 \cos\left(4\pi\frac{z}{a}\right)$$

$$\frac{1}{\pi}\sum_{n=1}^{n=\infty} b_n(-1)^n R_{3n}(z) + \frac{1}{\pi}\sum_{m=1}^{m=\infty} a_m(-1)^{m-1} R_{4m}(z) = 0. \tag{32}$$

The above equations are solved using Schmidt method (Yau 1967). The stresses and the displacements obtained for $2a = R$, $\delta_1 = 0{\cdot}1R$ and $\delta_2 = 0{\cdot}1\delta_1$ are plotted in figure 6a.

The deformed surface and subsurface profiles are also shown in figure 6b for $R = 1, 2a = R, \delta_1 = 0{\cdot}1R, \delta_2 = 0{\cdot}5\delta_1$.

4. Conclusion

The contact of rough surfaces was studied at micro and macro scales. The results provided better understanding of the contrasting nature of the rough contacts at different scales. Micro contact mechanics provided a means for predicting potential sites for crack nucleation while macro contact mechanics enabled predicting subsequent fracture and plasticity activity in the near surface vicinity. The length scales differed by well over two orders of magnitude making it important to study micro and macro contact mechanics separately before attempting unified numerical evaluation.

References

Conway H D, Farnham K A 1967 Contact stresses between cylindrical shafts and sleeves. *Int. J. Eng. Sci.* 5: 541–544

Hills D A, Nowell D, Sackfield A 1993 *Mechanics of elastic contacts*. (Oxford: Butterworth-Heinmann)

Johnson K L 1985 *Contact mechanics*. (Cambridge, UK: Cambridge University Press)

Maugis D 2000 *Contact, adhesion and rupture of elastic solids*. (Germany: Springer)

Rajendrakumar P K, Biswas S K 1996 Elastic contact between a cylindrical surface and a flat surface—A non-hertzian model of multi-asperity contact. *Mech. Res. Commun.* 23(4): 367–380

Spillers W R 1964 A shrink fit problem. *J. Math. Phys.* 43: 65

Tranter C J, Craggs J W 1945 The stress distribution in a long circular cylinder when a discontinuous pressure is applied to the curved surface. *Philos. Mag.* 36: 241–250

Yau W F 1967 Axisymmetric slipless indentation of an infinite, elastic cylinder. *SIAM J. Appl. Math.* 15(1): 219–227

Yau W W F, Cakmak A S 1966 The indentation problem of an infinite, hollow, elastic cylinder for an axisymmetric punch of finite length and arbitrary profile. *Int. J. Eng. Sci.* 4: 463–481